encit 2020

ABCM
Associação Brasileira de Engenharia e Ciências Mecânicas

18th Brazilian Congress of Thermal Sciences and Engineering
November 16–20, 2020 (Online)

ENC-2020-0327
EXPERIMENTAL AND NUMERICAL EVALUATION OF FLUID DISPLACEMENT IN A NARROW ANNULAR

Otávio A. Verhagem
Fernando G. Mazzuchetti
Diego M. M. Silva
Nezia de Rosso
Cezar O. R. Negrão
Federal University of Technology-Parana - UTFPR. Rua Deputado Heitor Alencar Furtado, 5000 - Bloco N - Ecoville - CEP 81280-340. Curitiba / PR - Brasil
otaviov.cernn@gmail.com, fgbur84@gmail.com, diego.munardessilva@gmail.com, nezia.rosso@gmail.com, negrao@utfpr.edu.br

Abstract. *The present work seeks to explore, experimentally e numerically, the effect of flow in the efficiency of the fluid displacement using Newtonian fluids in a narrow annular. In order to evaluate the efficiency experimentally an experimental rig was built. The test section is composed of 2 stainless steel pipes with 5.7 m length. The inner pipe has an external diameter of 0.089 m while the external pipe has an internal diameter of 0.102 m. The acquisition system allows the evaluation of fluid displacement in real time. The experimental rig was able to capture the fluid displacement by analysis of the pressure and density signals over time. As a whole, these signals allow to evaluate the efficiency of the process of removing the displaced fluid. Results show a decrease in efficiency with the increase in flow rate. The same tendency is observed in the numerical results, where it was observed that when the flow rate is increased the displacing fluid tends to penetrate into the displaced fluid.*

Keywords: *fluid displacement, experimental, numerical, efficiency, narrow annular.*

1. INTRODUCTION

Primary cementing is considered one of the most critical stages of the oil well drilling process (Derviş, 2013). Its main objective is to promote, through the use of cement, the insulation between formation and well, thus creating a hydraulic seal. In addition, it is responsible for ensuring the stability and structural strength of the well (Nguyen and Usher). Problems and failures in this process caused, mainly, by the deficient displacement (Holt *et al.*, 2013) can generate negative economic and environmental impacts, such as the reduction of the maximum production potential and instability of the well. Additionally, corrective treatments can extend the process from 1 to 2 days.

The efficiency of fluid displacement in primary cementing is influenced by parameters such as, flow rate, rheology, density ratio between displaced and displacing fluid. In addition, the centralization and movement of the casing string can also improve the efficiency (Haut and Crook, 1979; Hossain and Islam, 2018). The eccentricity between casing and the drill pipe tends to make the cement slurry flow only through the wider part of the annular, not allowing the displacement in the narrow part (Haut and Crook, 1979; Jakobsen *et al.*, 1991).

Viscosity is another important parameter, which characterize the flow resistance of a fluid. As observed by (Dutra *et al.*, 2005), it is important to have a viscosity hierarchy, where a less viscous fluid should be displaced by a more viscous one. If this condition is not achieved, a tendency of interpenetration between the two fluids can be observed, and, as a consequence, a decrease in efficiency is noticed (Tardy and Bittleston, 2015). Similar behavior also was noticed for densities (Tehrani *et al.*, 1992). The hierarchies promote more stability in the interface of displacement (Tardy and Bittleston, 2015).

A tendency to improve efficiency also was observed by (Aranha *et al.*, 2012; Couturler *et al.*, 1990; Haut and Crook, 1979) with higher flow rates, especially for turbulent regimes and wide annular. However, in narrow annular, reaching the turbulent regime becomes a complex task. A greater pressure gradient at the bottom of the well is necessary, which can result in fracture of the formation. (Zulqarnain and Tyagi, 2016) observed that for the turbulent regime it is necessary to pump more volume of displacing fluid to complete the displacement, which decreases the efficiency.

Due to the complexity involved with the phenomena during fluid displacement, a numerical approach has been an alternative to understand mechanisms that are not possible to visualize experimentally. (Szabo and Hassager, 1997) used a 3D simulation based on Euler-Lagrange approach to model the behavior of the interface between the two fluids during displacement. They based their analysis on a Froude number. It was observed that for Froude numbers greater than 1 the

inertia forces dominate the interface. This effect causes a tendency of displacing fluid channeling in displaced fluid. On the other hand, values lower than 1 indicate a flatter interface.

As observed, the fluid displacement in a wide annular is quite comprehensive, describing several phenomena involved both experimentally and numerically. However, there is still a lack of studies that seek to understand whether the same phenomena apply to narrow annular in laminar regimes. Given this, the objective of the present work is to explore, experimentally and numerically, the effect of flow variation on the efficiency of Newtonian fluid displacement in a narrow and concentric annular.

2. Methodology

2.1 Experimental unity

In order to evaluate the efficiency of fluid displacement in vertical wells, an experimental device was built. It consists of a hydraulic, mechanical and data acquisition system, as illustrated in Fig. 1.

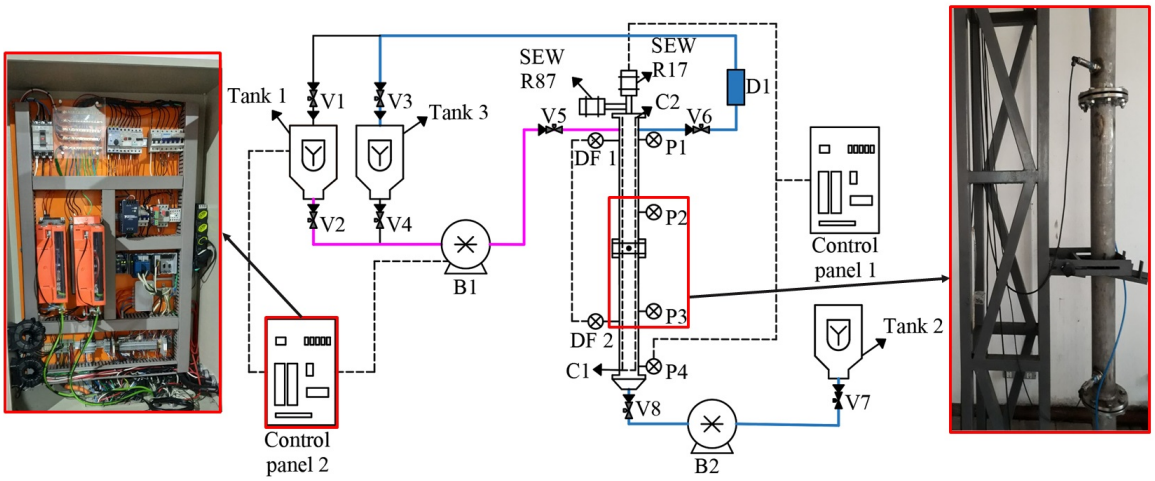

Figure 1. Experimental rig schematic. First image shows the control panel, responsible to operate the valves and pumps. The second image summarizes the experimental setup and shows the path of fluids 1 and 2 in pink and blue, respectively. The third image shows the actual setup, two transducer are observed plugged in the $0.089\ m$ outer tube.

The hydraulic system consists of one test section, 2 pumps (B1 and B2), 8 valves (V1, V2...V8) and 3 tanks, as shown in Fig.1. The section test is made with two stainless steel pipes with height $L = 5.7\ m$ and annular geometry. The tube representing the formation has an inner diameter of $D_i = 0.102\ m$, and the tube representing the casing has an outer diameter of $D_e = 0.089\ m$. The B1 is a helical pump and it is used for fluid 1 (displaced fluid) circulation. It is capable of reaching $2.777 \cdot 10^{-3}\ m^3/s$ flow rate and pressure of $12 \cdot 10^5\ Pa$. On the other hand, the B2 pump is a peristaltic pump that is responsible for pumping fluid 2 (displacing fluid) from the bottom of the annular, and can reach flow rate up to $2.777 \cdot 10^{-4}\ m^3/s$ and pressure up to $4 \cdot 10^5\ Pa$. The electropneumatic ball valves (V1 to V8, Fig.1), give direction to the fluid as needed. Finally tank 1 is used for fluid 1 storage, tank 2 for fluid 2 storage and tank 3 for decanting and storing fluids after testing.

In the mechanical system there are two SEW EuroDrive® servo motors. One of them is for axial displacement control that allows the reciprocation, insertion or removal of the casing string (SEW R87, Fig.1). The other one is responsible to rotate the inner tube up to 100 RPM (SEW R17, Fig.1). In addition, adjustable spherical positioners are distributed in 2 points of the test section (C1 and C2) and guarantee eccentricity from 0 to 100%.

The data acquisition system consist of 5 pressure transducers distributed through the test section, which are used to map the interface during the substitution. Being 4 of them absolute pressure, from 0 to $6 \cdot 10^5\ Pa$ (P1 to P4, Fig.1), with precision class 0.05% and 1 differential pressure, from $-1 \cdot 10^5$ to $2 \cdot 10^5\ Pa$ (DF1 and DF2, Fig.1). In addition, a densimeter (D1) coupled to a mass flow meter installed at the outlet of the experimental unit provides auxiliary data for understanding the phenomenon.

The control and data acquisition is done through the National Instruments® CompactDAQ, along with a routine developed internally in LabView software®. Through a computer connected to control panel 2 (Fig.1), this system allows remote control hydraulic pumps, valves, and servo motors, as well as recording and displaying in real time the data from the tests.

2.2 Fluid properties

To evaluate the influence of the physical properties of fluids on the fluid displacement, two Newtonian fluids were used to perform the tests. Fluid 1, soybean oil with viscosity $0.062\ Pa \cdot s$ and density $890\ kg/m$, represents the drilling mud (displaced fluid). Fluid 2, a glucose syrup solution in water with viscosity $0.106\ Pa \cdot s$ and specific mass $1310\ kg/m$, represents cement slurry (displacing fluid).

2.3 Methodology

The testing procedure is standardized, following a sequence of steps so that all experiments are performed under the same conditions. For the beginning of the test protocol, fluids 1 and 2 are homogenized in their respective tanks by mixer. In the sequence, valves V1, V3, V5 and V6 are opened and pump B1 is triggered, filling the pipe and annular with fluid 1. Pumping is done until the stabilization of its pressure curve and specific mass, ensuring the complete filling of the pipe with fluid 1 (line 2, Fig.1). For the start of the fluid displacement, valve V1, V3 and V5 are closed, the valves V2, V7 and V8 are opened and pump B2 is switched on, initiating fluid 2 pumping from the bottom of the annular and directing the flow to the tank 3. The range of Reynolds number used in the tests was 4 to 21 for the glucose solution and from 6 to 35 for the oil. During fluid displacement, densimeter and differential transducers are monitored. The pump remains on until the densimeter values correspond to the fluid 2 density.

2.4 Numerical model

The numerical domain represents only the testing section of the experimental unit, as it is the region of interest to analyze the development of the interface. Figure 2 shows the modeling of the annular domain with outer diameter $D_e = 0.102\ m$ and inner diameter $D_i = 0.089\ m$. A total length of $L = 2\ m$ is used, as shown by (Szabo and Hassager, 1997) the efficiency of the substitution tends not to be influenced by the ratio between the well height and the gap for values much greater than 1. This allowed a greater refining of the mesh without considerably increasing the computational cost. At the bottom, a space with $D_e = 0.102\ m$ in external diameter and $0.05\ m$ height represents the region before the beginning of the steel casing as occurs also in the experimental unit. It is also considered a laminar and isothermal flow for the whole domain. Newtonian fluids with the same experimental properties are used.

The governing equations are discretized by using the element-based finite volume method and solved by employing the CFD package Ansys ® CFX ® in its 2019 R3. The homogeneous Euler-Euler model is used to solve the liquid-liquid flow. In this model, boths phases are treated as continuous and average conservation equations are solved as a mixture or a bulk (ANSYS Inc., 2019). As boundary conditions, the entry into the lower region was defined as an specified mass flow. The walls are treated as no slip walls and the end on the top of the testing section is treated as opening with relative opening pressure of $0\ Pa$.

The 3D mesh composed of hexahedral structured elements presented in Fig. 2 was generated through the software Ansys® ICEM CFD™. To ensure that the results were not influenced by the mesh, a sensitivity test was also done with six meshes, refined uniformly in the axial and radial directions, with increments of approximately 50% in the number of divisions per element. As convergence criteria is used Root Mean Square (RMS) of the equations of mass conservation and momentum with values equal to 10^{-5}. As a comparison criterion, the values of the velocity profile in a developed flow region, the pressure gradient between the input and output region of the domain and the volume fraction were used. Finally, a convergence of the results was observed from mesh 4, in which the variation was around 3% as compared with the most refined mesh.

2.5 Dimensionless numbers

To evaluate the results, three dimensionless numbers were used, Reynolds number, Buoyancy number and Froude number. The Reynolds number evaluates the ratio between inertial and viscous forces and is also used as a parameter to indicate the fluid flow regime. Reynolds number is calculated through Eq. 1,

$$\mathbf{Re_i} = \frac{\rho_i \cdot \overline{v} \cdot h}{\mu i}, i = 1, 2 \tag{1}$$

where ρ is the density of the fluid, $h = R_{outer} - R_{inner}$, h is the annular gap, R_{outer} is the outer radius and R_{inner} is the inner radius, $\overline{v}$ is the average velocity of the flow, μ the fluid viscosity and i specifies the fluid used.

The Buoyancy number relates the inertial with buoyancy forces and it is calculated using Eq. 2.

$$\mathbf{Bu}\frac{(\rho_1 - \rho_2)gh^2}{\overline{v}\mu_1} \tag{2}$$

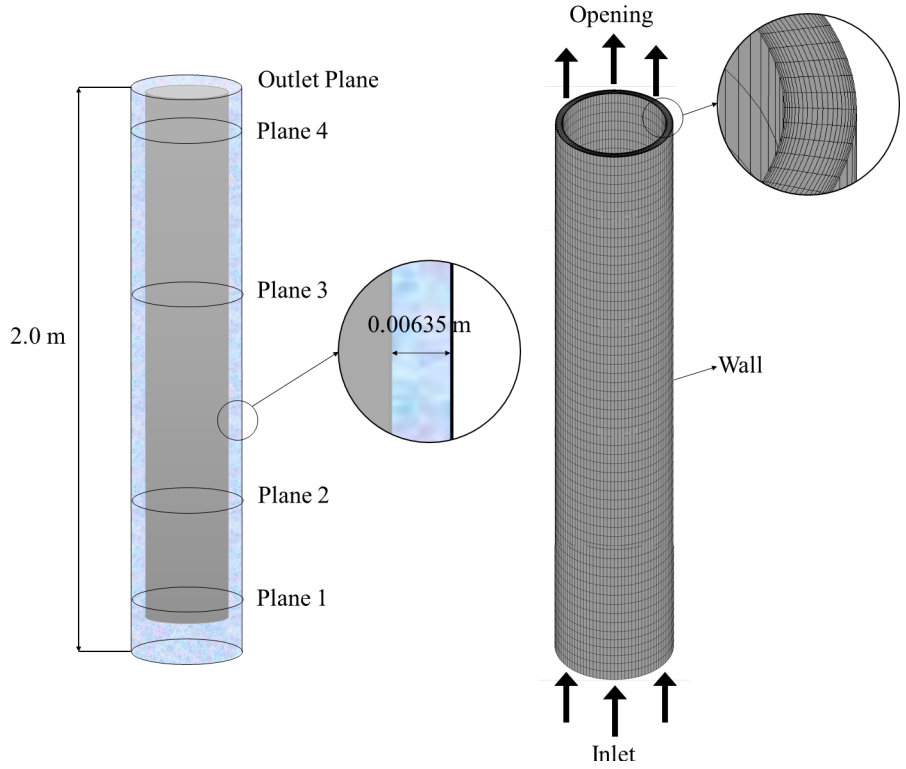

Figure 2. Modeling the fluid domain of the testing section. Left is a schematic of the model. Total high is 2 m, Plane 1 is 0.1 m, Plane 2 is 0.48 m, Plane 3 is 1.02 m and Plane 4 is 1.9 m from the inlet plane. Right is the mesh used in the numeric model with the boundary conditions.

where g is the gravity acceleration, ρ_1 is the density of the fluid displaced and ρ_2 is the density of the fluid discpaling

The Froude number is given by the ratio between the two dimensionless numbers, Reynolds number and Buoyancy number, as shown in Eq. 3.

$$\mathbf{Fr} = \frac{Re_1}{Bu} \tag{3}$$

3. RESULTS

In this section, the numerical and experimental results for fluid substitution in narrow concentric annular are presented.

Figure 3 shows a result of a test for flow rate of $6.944 \cdot 10^{-5}\ m^3/s$ that will be used to show the main points to be analyzed during the fluid displacement tests. The black curve corresponds to the differential pressure results and the green one corresponds to the density results. The other items will be used for complementary information. Items from "1" to "5" and from "a" to "e" from Fig. 3 will be used during the explanation of the results. It is possible to observe a delay between the differential pressure and density curves between the item "1" and "5". This occurs because the data is obtained at different points as presented in Fig. 1.

The Differential Pressure curve is obtained through the differential transducers (TD1 and TD2), shown in Fig.1 installed at point 1, 1.25 m, and pont 2, 5.25 m, from the bottom of the wel, respectively.

The analysis of the density is done in a similar way, the volume count is made from the beginning of the test in line "a", and is finished when reaching the density of fluid 2 in the densimeter represented by line "d".

In addition, another parameter to be observed is the breakthrough time of the interface (when the first signal of fluid 2 is detected at a certain point). For the results, the volumes will be observed when achieving the first differential transducer in 1.25 m this corresponds to 0.00337 m^3. It will also be considered when the volumes achieve the densimeter after the exit of the experimental unit with a volume of 0.018 m^3. These volumes are represented by the vertical lines "Bt 1" for the differential transducer and "Bt 2" for the densimeter. According to Zulqarnain and Tyagi (2016), the presence of fluid 2 before the breakthrough line indicates interface interpenetration.

Exploring the differential pressure curve, the beginning of fluid 2 pumping is observed in 1 (Fig. 3). The horizontal line at the beginning indicates that there is still fluid 1 passing through the transducer "TD1". The slope of the curve, indicated by 2, shows the progression of the interface on the annular. An increase in the differential pressure is observed by increasing the volume fraction of fluid 2 in this section. Because it is both higher viscosity and density, the pressure drop in its displacement is greater, which results in a higher pressure necessary for its flow to occur. The differential

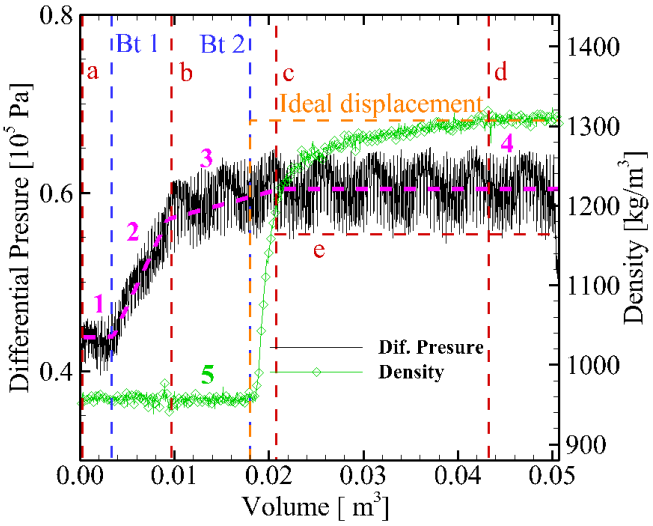

Figure 3. Example result with intermediate flow rate $6.944 \cdot 10^{-5}\ m^3/s$. The black curve corresponds to the differential pressure results and the green one corresponds to the density results, the other items shows the main to be observed.

pressure stabilizes when the section is filled with fluid 2, shown by the plateau of item 4.

When analyzing the results of Fig. 3 it is possible to observe a second slope between lines "b" and "c", indicating a difficulty in the final stages of fluid displacement. This effect is evident in Fig. 4 "d". Table 1 presents the volumes required to complete each step of the fluid displacement. The column "Total Densimeter Volume" corresponds to the volume between lines "a" and "d", "Annular Volume 1" corresponds to the volume between lines "a" and "b", "Annular Volume 2" is the volume between lines "b" and "c" and "Total Annular Volume" is the sum of volumes 1 and 2. It is possible to observe that the volume required to complete the second stage of substitution tends to get larger with the increase in flow rate, resulting in a decrease in the efficiency of the fluid displacement. In addition, there is a considerable increase in the total volumes required to complete the substitution, also indicating a decrease in the total efficiency of the fluid displacement.

Table 1. Compilation of volumes required during the experimental tests for fluid displacement for four different operational condition.

Flow rate	Total Densimeter Volume	Annular Volume 1	Annular Volume 2	Total Anullar Volume
$6.944 \cdot 10^{-5}$ [m³/s]	0.0312 [m³]	0.0105 [m³]	0.0201 [m³]	0.0306 [m³]
$1.388 \cdot 10^{-4}$ [m³/s]	0.0420 [m³]	0.0102 [m³]	0.0258 [m³]	0.0360 [m³]
$2.088 \cdot 10^{-4}$ [m³/s]	0.0431 [m³]	0.0101 [m³]	0.0331 [m³]	0.0432 [m³]
$2.777 \cdot 10^{-4}$ [m³/s]	0.0526 [m³]	0.0106 [m³]	0.0359 [m³]	0.0465 [m³]

It is possible to observe through the density data in Fig.3, that initially at the horizontal level of values indicated in 6, only fluid 1 flow is occurring. At the point indicated by line "c", fluid 2 is captured by the densimeter, and a sudden increase in the sensor reading is observed up to the horizontal line "e". This shows a behavior close to the ideal displacement line. After this point the density values move away from the ideal curve, demonstrating a mixture between the two fluids, as well as indicating the differential pressure data. Through the breakthrough lines in Fig. 4, it is possible to observe that up to the flow of $1.388 \cdot 10^{-4}\ m^3/s$, the beginning of the flow of fluid 2 through the first transducer coincides with the Bt 1. For flows above $2.088 \cdot 10^{-4}\ m^3/s$, it is noted that fluid 2 reaches the line of the first transducer before the Bt 1, indicating channeling. The same fact is confirmed by observing the density data, given that for low flow rates of fluid 2 is detected slightly after line Bt 2, and for higher flow rates the interface reaches the densitometer before the line of breakthrough.

To help understanding the phenomenon, numeric results were used to visualize the interface behavior with the increase of the flow rate. Figure 5 shows the volume fraction contour of fluid 2, plotted on a plane that cut the domain in the middle. Each item from the figure, where ($a = 6.944 \cdot 10^{-5}\ m^3/s; b = 1.388 \cdot 10^{-4}\ m^3/s; c = 2.088 \cdot 10^{-4}\ m^3/s; d = 2.777 \cdot 10^{-4}\ m^3/s$), represents only one side of the annular from the same point (rectangle), since the case studied is concentric annular there are no differences between the sides of the gap. It is possible to observe that for flow rates of $6.944 \cdot 10^{-5}\ m^3/s$ until $1.388 \cdot 10^{-4}\ m^3/s$ the interface remains practically flat. However, for flows of $2.088 \cdot 10^{-4}\ m^3/s$ until $2.777 \cdot 10^{-4}\ m^3/s$, a tendency of channeling fluid 2 within fluid 1 is observed.

Figure 6 (a) presents the numerical results for differential pressure calculated from the difference between the pressure average of planes 4 and 2 shown in Fig. 2. Figure 6 (b) shows the volume fraction averages in planes 1, 2, 3 and in the

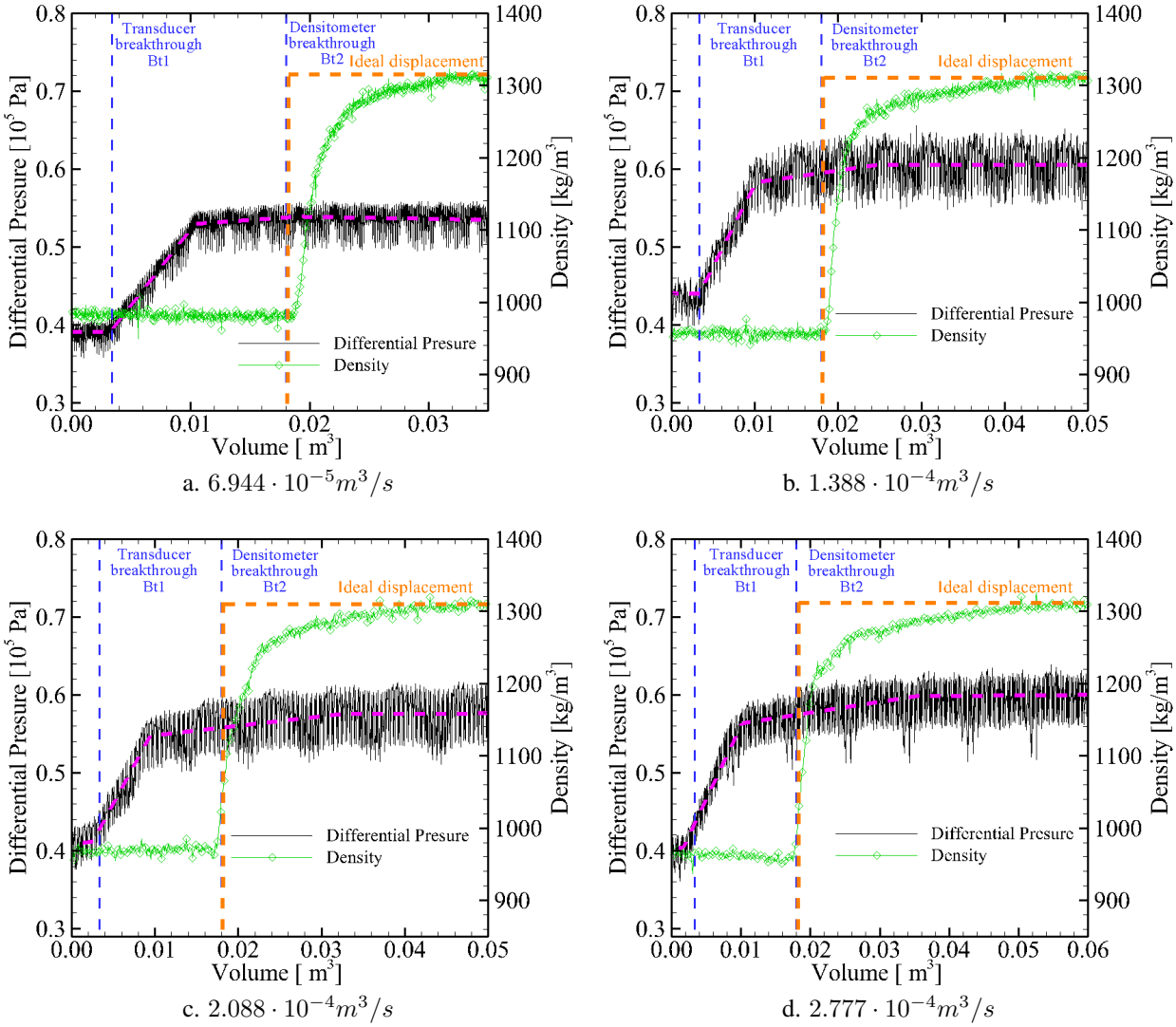

Figure 4. Experimental results of fluid displacement for four flow rates, a. 0.0312 m^3; b. 0.0420 m^3; c. 0.0431 m^3; d. 0.0526 m^3. In a. and d., low flow rates, interpenetration at the interface is not observed in comparison with the breakthrough lines. However for tests c. and d., fluid 2 is observed before the breakthrough lines, indicating interpenetration at interface. In addition, the volume to conclude the displacement increases as the flow rate increase.

output of the numerical model for the same 4 flow rates shown in the legend of Fig. 6 (a). Vertical lines represent the breakthrough lines for their respective planes. It is possible to see that the numerical simulation can represent the behavior observed on experimental tests, especially for the flow rate of $2.7 \cdot 10^{-4}$ m^3/s where fluid 2 passes through the output plane long before its respective breakthrough line. It is also noted, through volume fraction mapping, that there is an increase in channeled volume with the fluid progression inside the annular, especially at the highest flow rate.

One way to evaluate the observed phenomenon is by comparing the Froude numbers for each flow rate. Table 2 shows the values of Reynolds, Buoyancy and Froude for the tests performed. It is observed that, in the low flow rates ($6.944 \cdot 10^{-5}$ m^3/s), the Froude number is < 1. According to the literature, this indicates that the interface tends to be flat, not presenting interpenetration between the fluids. This is reflected both in the experimental results and in the numerical results presented previously. For high flow rates, the Froude number begins to assume values > 1 indicating the interpenetration trend in the interface. It is interesting to note that for a Froude number very close to 1 for the flow rate of $1.388 \cdot 10^{-4}$ m^3/s, there were no expressive reflexes of the effects of the canalization when compared to the case of lower flow, it is also possible to observe that the volumes needed for displacement were similar. In cases where the Froude number becomes a slightly higher than 1, the effect of channeling becomes expressive. It is observed that this hypothesis corroborates with the numerical results. This phenomenon can be confirmed by observing the experimental results in the breakthrough, becoming an alternative to predict the loss of efficiency in the fluid substitution in narrow annular.

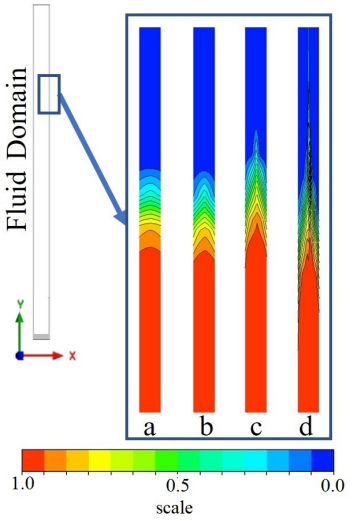

Figure 5. Color maps of the interface behavior as a function of flow rate: a. $6.944 \cdot 10^{-5} m^3/s$; b. $1.388 \cdot 10^{-4} m^3/s$; c. $2.088 \cdot 10^{-4} m^3/s$; d. $2.777 \cdot 10^{-4} m^3/s$. The colors, from red to blue indicate the volume fraction of the Fluid 2 during the fluid displacement. As the flow rate increases the interpenetrating behavior of the interface increases

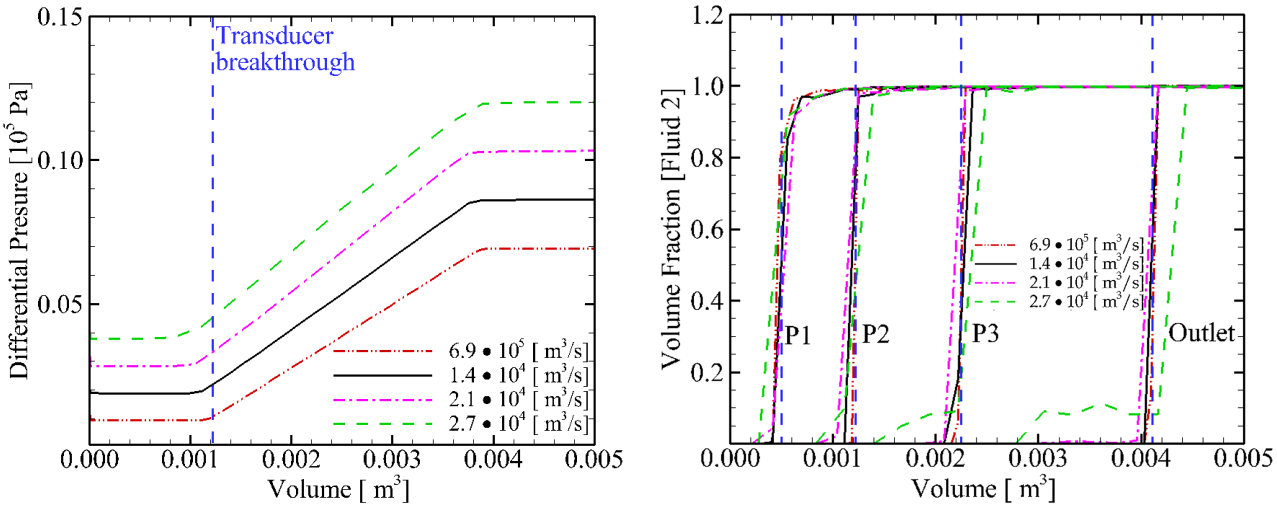

a. Differential dynamic pressure

b. Volume fraction

Figure 6. Numerical newtonian fluid results: Figure a shows the interpenetrating behavior of the interface, which is similar to observed in the experimental results. Figure b shows that for higher flow rates, the interpenetrating volume tends to increase as the flow goes trough the annular.

Table 2. Reynolds, Buoyancy and Froude numbers used analyze the behavior of the interface

Flow rate	Reynolds	Buoyancy	Froude
$6.944 \cdot 10^{-5}$ [m³/s]	4.14	12.58	0.33
$1.388 \cdot 10^{-4}$ [m³/s]	9.65	8.12	1.19
$2.088 \cdot 10^{-4}$ [m³/s]	15.37	5.94	2.59
$2.777 \cdot 10^{-4}$ [m³/s]	21.17	4.67	4.59

4. CONCLUSIONS

This work presented numerical and experimental studies on the influence of flow rate increasing on fluid substitution in narrow and concentric annular. In contrast from what has already been studied in the literature for wide annular, it was demonstrated that increasing the flow rate in narrow annular tends to decrease the efficiency of substitution, especially for higher flow rates. It was also observed that a considerable increase in fluid 2 volume was necessary to complete the

displacement at higher flow rates. The numerical model adopted represents well the phenomenon observed experimentally while corroborating the hypothesis that the channeling of the fluid decreases the efficiency of the displacement. The proposed numbers seem to generalize the phenomena studied facilitating the analysis, and make it possible to evaluate the behavior of the interface during the fluid displacement. For higher Froude numbers, close to 1, the interface does not have a considerable channeling effect. However, for higher values, there was considerable channeling. In addition, the channeled volume tends to increase over the flow to higher flow rates.

5. REFERENCES

ANSYS Inc., 2019. "CFX-Solver Manager User's Guide".

Aranha, P.E., De Miranda, C.R., Cardoso, W.F., Campos, G., Martins, A.L., Gomes, F.C., Araujo, S.B. and Carvalho, M.S., 2012. "A comprehensive theoretical and experimental study on fluid displacement for oilwell-cementing operations". *SPE Drilling and Completion*, Vol. 27, No. 4, pp. 596–603.

Couturler, M., Gulliot, D., Hendriks, H. and Cailet, F., 1990. "Design rules and associated spacer properties for optimal mud removal in eccentric annuli". *Annual Technical Meeting, ATM 1990*, pp. 1121–1128.

Derviş, B., 2013. *Well cementing book*. Schlumberger, Sugar Land, Texas, 2nd edition.

Dutra, E.S., Martins, A.L., Miranda, C.R., Aragão, A.F., Campos, G., Mendes, P.R. and Naccache, M.F., 2005. "Dynamics of fluid substitution while drilling and completing long horizontal-section wells". Vol. 2005-June.

Haut, R.C. and Crook, R.J., 1979. "Primary cementing: The mud displacement process". In *Proceedings - SPE Annual Technical Conference and Exhibition*. LasVegas, Nevada.

Holt, C., Lahoti, N. and Fortier, V., 2013. "Dynamic cementation: A solution to well integrity problems". In *SPE/IADC Drilling Conference, Proceedings*. Vol. 1, pp. 634–641.

Hossain, M.E. and Islam, M.R., 2018. *Drilling Engineering Problems and Solutions*. Scrivener Publishing, 1st edition.

Jakobsen, J., Sterri, N., Saasen, A., Aas, B., Kjosnes, J. and Vigen, A., 1991. "Displacements in eccentric annuli during primary cementing in deviated wells". In *Production Operations Symposium*. Oklahoma City, Oklahoma.

Nguyen, T.T. and Usher, C., ???? Master's thesis, Norweigian University of Science and Technology, Trondheim, Norway.

Szabo, P. and Hassager, O., 1997. "Displacement of one Newtonian fluid by another: Density effects in axial annular flow". *International Journal of Multiphase Flow*, Vol. 23, No. 1, pp. 113–129.

Tardy, P.M. and Bittleston, S.H., 2015. "A model for annular displacements of wellbore completion fluids involving casing movement". *Journal of Petroleum Science and Engineering*, Vol. 126, pp. 105–123.

Tehrani, A., Ferguson, J. and Bittleston, S.H., 1992. "Laminar displacement in annuli: A combined experimental and theoretical study". *Proceedings - SPE Annual Technical Conference and Exhibition*, Vol. Delta, pp. 191–202.

Zulqarnain, M. and Tyagi, M., 2016. "Development of simulations based correlations to predict the cement volume fraction in annular geometries after fl uid displacements during primary cementing". *Journal of Petroleum Science and Engineering*, Vol. 145, pp. 1–10.

6. RESPONSIBILITY NOTICE

The author(s) is (are) solely responsible for the printed material included in this paper.